Fiber energy efficiency Part II: Forces acting on the refiner bars

Anders Karlström and Karin Eriksson, Chalmers University of Technology, Göteborg, Sweden

KEYWORDS: Refining models, Energy efficiency, fibre distribution, fiber network, pulp consistency, dynamic viscosity.

SUMMARY: In this paper it is shown that the defibration and fibrillation work in thermo mechanical pulp refiners can differ significantly dependent on the process conditions. This has a direct impact on the distributed force in the refining zones obtained when the bars hit the fibers or fiber bundles. The distributed force, which is defined as a vector along the surface of the refining segments, is estimated using a model where the total work can be split into reversible and irreversible work. Besides traditional refiner variables such as motor load, dilution water added and inlet- and casing pressures, measurements of temperature profiles in the refining zone and plate gaps from a full-scale CD-refiner are available as inputs. Three data sets are analyzed and it is shown that the shape of the temperature profile and the force distribution vary significantly. This means that the fiber distribution in the refining zone varies as well which affect the final development of the pulp properties.

The refining segment pattern and taper play an important role when estimating the force distribution and it is stated that the force distribution close to the contraction part of the flat zone as well as the outer part of the conical section are larger than in other positions. Therefore, specific energy which can be seen as the integral of the total energy distribution along the refining segments cannot be used when describing the variations in the distributed forces.

ADDRESSES OF THE AUTHORS:
Anders Karlström (anderska@chalmers.se)
Karin Eriksson (karin.eriksson@cit.chalmers.se)

Introduction

During the late 1980s, Miles and May (1990, 1991) derived a theoretical model of the pulp flow behavior in the refining zone of a high consistency (HC)-refiner. It became widely used and established a theory that increased the understanding of refining. The theoretical approach was to determine the radial pulp velocity and residence time based on calculations of the forces that affect the flow conditions. From this model the number of fiber impact per bar was derived.

Miles and May (1990, 1991) also introduced the concept of refining intensity which was defined as the ratio between the specific energy, i.e. the relation between motor load and the assumed production rate. The idea was to define a scalar which describes the bar-to-fiber impact estimated for the entire refining zone.

In those days, it was claimed that the specific energy is important to control. It was assumed directly related to the refining intensity and the pulp quality. This is the common strategy also today but as stated by Hill et al. (1993), problems arise if relying on specific energy alone not at least regarding variations in chip feed properties and errors when estimating production rates. Several studies had earlier pointed out the limitations of such strategies as well, see Hill et al. (1979), Johansson et al. (1980), Dahlqvist and Ferrari (1981), Oksum (1983), Honkasalo et al. (1989). This knowledge was later on used by Eriksen et al. (2008) who pointed out that the specific energy is a mean value of the distributed forces acting upon the pulp.

Moreover, Sabourin et al. (2001), claimed that the model derived by Miles and May (1990, 1991) is not suitable for practical use since it has too many unknown parameters and variables. One example was the friction coefficients introduced to describe the interaction between the refining segment surface and the pulp. Isaksson et al. (1997) had shown this statement earlier and concluded that the proposed friction coefficients are far from the values estimated in full-scale refiners and that the coefficients varied dramatically for different refining conditions.

In most work presented in pulp and paper journals, the friction coefficient is considered as a scalar having the same value in the entire refining zone. This approach is too simplified and imposes severe limitations when introducing more advanced modeling strategies. Some factors that influence the conditions are the material itself which changes along the radius. Temperature, consistency and pulp and steam velocities, as well as geometric parameters such as the pattern of refining segments and many other specific conditions will also affect the friction. Models based on such friction concepts are not suitable for comparison of different defibration/fibrillation conditions and it would be more appropriate to characterize the friction coefficients as system properties instead.

In search for a new refining intensity measure Kerekes (2011) proposed to link the intensities directly *"to the key variable causing the refining effect – forces on fibres"*. Kerekes also concluded that the force, not energy, should constitute the characterization of refining intensity. This is natural as an integrated measure of the energy distribution in the refining zone does not provide information of local refining conditions which is of importance for the final pulp characteristics. This was also in line with the results presented by Karlström and Koebe (1993) and later strengthened by Eriksson and Karlström (2009) where it was

shown that refining zone temperature profiles outperform the specific energy, primarily due to the spatial dynamic information obtained in the refining zone. Kerekes (2011) approach is also supported by results provided by Backlund et al. (2003) who showed that the variations in the shear force distribution in the refining zone are considerable which undoubtedly will affect the final pulp properties. Unfortunately, the refining intensity measure developed by Kerekes (2011) lack spatial information and it is also based on the same approach regarding friction coefficients as introduced by Miles and May (1990, 1991).

To find a new measure for the refining intensity vector, Karlström et al. (2008) derived a model based on a rheological approach where the friction forces, used by Miles and May (1990, 1991) as important variables, were excluded from the derived set of material and energy balances. Eriksson (2005) and Karlström et al. (2008) proposed that the fluid friction should be seen as an internal resistance described by the shear stress and shear rate as these physical variables can be derived for different refining conditions.

Huhtanen (2004) used a physical approach as well and described the flow of concentrated fiber-water-steam suspensions inside refiner grooves, suspensions in pipes and mixing tanks near a rotating disc. The results were promising and from a fluid mechanics perspective, the introduction of the total shear stress is motivated.

The model developed by Karlström et al. (2008) included a possibility to split the motor load into thermodynamic work associated with the steam generation and the irreversible work related to the defibrations/ fibrillation of the fiber. It was shown that the derived distributed irreversible work together with specific machine parameters is suitable for energy distribution studies, see Karlström (2013). The model, which is often called the entropy model, can be seen as a macro model that should be linked to a micro model describing local phenomena when the refining bars and grooves interact with the fiber bundles.

This paper is in line with Kerekes (2011), ideas to broaden the discussion how to formulate future energy efficiency concepts based on forces acting on the fiber bundles when they are defibrated and fibrillated between the refining bars. Therefore, in this paper, the extended version of the entropy model derived by Karlström and Eriksson (Part I, 2014) will be used when estimating the force distribution along the segment length. To estimate the energy distribution at different process conditions, process data from a commercial full-scale CD-refiner is used. The concept of fiber energy efficiency was introduced to describe the defibration and fibrillation work obtained when the fibers and fiber bundles interact with the refining bars. The main purpose was to distinguish between the energy distribution related to the thermodynamical work (steam generation) and the actual work on the fibers (i.e. the development of the fiber properties). This approach will also link to a paper by Ferritsius et al. (2014) where modeling aspects are discussed from a pulp characterization perspective.

This paper is the second in a series of four consecutive papers where the macro- and micro-modeling efforts form a multi-scale modeling concept.

Fundamentals

When deriving models including refining intensity measures it is necessary to introduce simplifications, especially if considering on-line applications. In this context, it is natural to mention the interesting work performed by Mohlin (2006) and Kerekes (2011) for low consistency (LC)-and HC-refiners. They introduced an empirical measure for the refining intensity and stated that the bar forces are linked to forces on fibers through fiber distribution over bars and gap size. Kerekes (2011) also formulated that

"Predictions of forces from this intensity were compared to forces measured in a high-consistency primary refiner, reject refiner, and a low-consistency refiner in mechanical pulping. The predicted and measured forces were in good agreement for the reject and low consistency refiner, and somewhat less so for the primary refiner."

Moreover, Kerekes and Senger (2006) use the Specific Edge Load (SEL) defined as the power supplied to the refiner divided by the product of the number of bars on the rotor, the number of bars on the stator, the length of working zone, and the rotational speed. In LC-refining this is a commonly used measure which has been used for many years to describe refining intensity, see Brecht and Siewert (1966). It was claimed by Kerekes (2011) that this measure is a good candidate to characterize refining intensity in LC-refiners. It was also indicated that SEL should be seen as a bar intensity that represents the energy expenditure at bar crossings. However, this refining intensity measure was an average over the refining segments and not spatially defined along the radius which is considered in this paper.

We are interested in the force exerted on fiber bundles and there are few sources of data for comparing the forces on individual fibers. Batchelor and Ouellet (1997) showed that the forces on a fiber in a bundle could vary from 0 to 0.2 N simply as a result of fiber orientation with respect to the bar edge. Kerekes and Senger (2006) estimate forces on fibers and found an approximate normal force on the fibers of 0.17 N for SEL = 2 J/m. In recent work, using a different approach, Lundin et al. (2008) predicted the shear force on fibers to be about 0.47 N in LC-refining.

All efforts to develop a deeper understanding of the refining intensity have been valuable and naturally, the development of new robust measurement technologies for placement inside the refining zone has been vital to meet future challenges. For instance, it is well known that a reduced plate gap can result in fiber shortening and this is of course related to the refining intensity. At a critical gap size the fiber length decrease sharply, see Mohlin (2006), most likely as a consequence of a fiber network collapse. In HC-refiners this statement was strengthened by Eriksson and Karlström

(2009), where fiber network collapse was indicated by comparing the force distributions of the axial thrust and the steam pressure inside the refining zone based on process data from a full-scale RTS-refiner.

Several research projects can be mentioned regarding measurements of local phenomena in the refining zone. Senger et al. (2004) measured the normal and shear forces of the fiber bundles between the stator and rotor bars while Eriksen et al. (2008) measured the pressure pulses obtained when the bars hit the fibers. The measurements performed were unfortunately only obtained from local positions in the refining zone and gave thereby limited information of the distributed properties.

The entropy model approach

To obtain more information about the distributed forces, the irreversible work derived from the entropy model, described by Karlström et al. (2008) and Karlström an Eriksson (Part I, 2014), can be a good starting point.

Consider an element in the defibration/fibrillation work vector, $w_{def}=8$ MW/m^2, at a radius $r=0.8$ m in a Twin refiner, see Karlström (2013), as obtained by the entropy model. The width of the refining bars is 3 mm while the width of the grooves is about 5 mm. In total, we have about 630 bars per revolution.

Assume that the bars capture the entire irreversible work derived by the entropy model, i.e. about $24 \cdot 10^3$ N/s,bar.

At 1500 RPM the compression time per bar will be about 0.05 ms which means that we get a force 1-2 N per bar at this radius. It is notable, that the force derived by the entropy model is comparable with the averaged shear and normal forces[1] in a HC-refiner obtained by Senger et al. (2004).

The segment pattern can differ considerably dependent on type of the refiner. A large full-scale primary refiner has normally more refining bars with smaller width compared with pilot refiners and it is important to characterize the number of bars at any given radius before estimating the forces. In short, a large number of bars mean most often reduced force impact on each bar at the same irreversible work at that position. This discussion can also be extended to understand the force distribution in a refiner zone. Consider Fig. 1 where a refining segment is divided into three sections called coarse, intermediate and a fine bar sections. As seen, the bar width is different in the three sections and so is also the length of the bars.

As a consequence of the possibility to estimate the irreversible work, the entropy model can provide more information about the spatial average bar-to-fiber interaction, i.e. the forces along the segment radius. By using the plate pattern, like the one given in Fig. 1, the forces acting on the bars in each section can be derived as a function of the radius. This is shown in Fig. 2 for a Twin disc refiner where the irreversible work varied about +/- 20 % which is indicated as upper and lower limits.

Too much variation in the estimated tangential forces, represented by the irreversible work in Fig. 2, should be avoided and Eriksson et al. (2010) indicated that a reduction in the temperature profile variations most likely reduce the variations in the irreversible work.

Dimension (mm)	FINE	INTERMEDIATE	COARSE
Bar width	4	5.5	7
Growth width	4	5.5	7
Zone length	90	90	100
Interval	840-930	750-840	650-750

Fig. 1: Example of a refiner segment which is divided into three sections with different segment pattern.
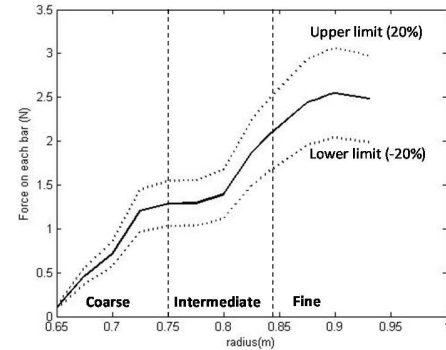

Fig. 2: Example of force on each bar as a function of radius in a refiner using the segments described in Fig. 1. These results are derived from the irreversible work obtained by the entropy model using mill data from a Twin refiner.

As described by Karlström and Eriksson (Part I, 2014), disturbances in the fiber network are highly dependent on the fact that steam can evacuate both forwards (towards the periphery of the segments) and backwards (towards the inlet) with a stagnation point at some radius in between, see Fig. 3. It is important to understand that the characteristics of the fiber network can change a lot as a result of changes in the process conditions and this will affect the pulp residence time. Moreover, the position for the stagnation point can vary significantly. This can be followed by measuring the temperature profile along the radius.

The maximum temperature (T_{max}) in Fig. 3 plays an important role as this peak implies a zero pressure gradient, $\partial P/\partial r$.

The disturbances can be caused by pumping effects which can be a consequence of variations in the local fiber pad density or by deliberated changes in for instance the production rate or the dilution water flow rate. All this will affect the force distribution along the refining zone and papers which give a good guideline of the intrinsic part of how the fiber fraction develops inside the refining zone are

---

[1] Note, the integral of the shear and normal forces in the measurements performed by Senger et al (2004) over a bar should be used in order to get a comparable measure with the force obtained from the entropy model, i.e.

the force related to the irreversible work is the sum of all forces in time acting on the fibers defibration/fibrillation during the bar-to-fiber impact.

written by Atack et al. (1984), Karnis et al. (1985) and Härkonen et al. (1999).

In this paper, the concept of distributed work and forces acting on the segment bars will be discussed in more details and complements the description given in Karlström and Eriksson (Part I, 2013).
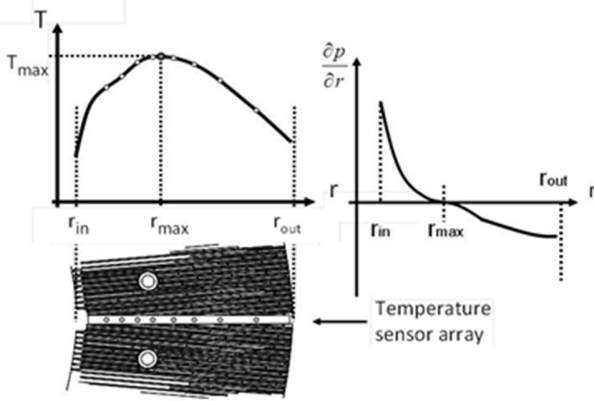

Fig. 3: A typical temperature profile from a primary refiner where a sensor array is placed between two refining segments.

Below, all data is based on a test series provided in a full-scale CD-refiner (CD82 running at 1800 RPM), see Fig. 4. Both refining zones, i.e. the flat zone and the CD-zone are equipped with temperature sensor arrays and plate gap sensors which open for estimations of the distributed forces using the entropy model.
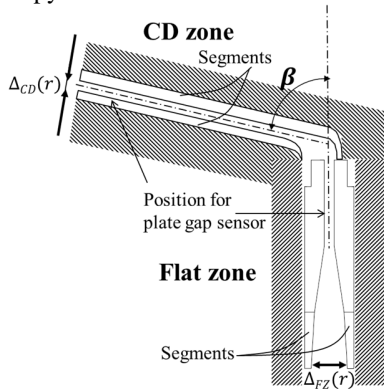
Fig. 4: A schematic drawing of the refining zones in a CD-refiner. The vertical flat zone is directly linked to the CD-zone via an expanding point.

The angle β between the flat zone and the conical zone, shown in *Fig. 4* is important to include in the entropy model as it affect the work distribution between the flat zone and the CD-zone. This is indicated in Fig. 5 where the ratio between the work in the flat zone and the total work, i.e. the motor load is given as a function of β which is different dependent on the CD-refiner design.

The ratio varies quite much between the upper and lower limits in Fig. 5 and depends on the refining conditions and how the fiber pad distributes on the refining surface.

A large angle β will increase the work performed in the flat zone and the shape of the curve in Fig. 5 is a consequence of the fact that the shear force estimation in the CD-zone must be modified to take the angle into account in the extended entropy model.

It is easy to show that the dynamic viscosity is an important variable together with the free variable α which is affected by the angle as well. This will be further discussed in consecutive papers in this series describing a more generic multi-scale modeling approach.
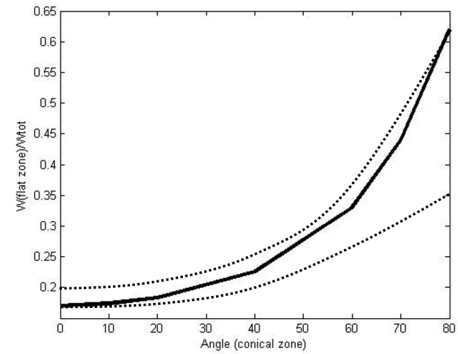

Fig. 5: Ratio between the work in the flat zone and the total work versus the angle β between the flat zone and the conical zone. Dotted lines indicates the upper and lower limits for the data series studied. The solid line indicates a snapshot in time.

Results and discussion

Consider a case when the production rate changes from 12.4 T/hr to 15.8 T/hr according to *Fig. 6*. The dilution water feed rates to the flat- and CD-zones are kept as stable as possible. Only minor fluctuations in the plate gaps are seen in Fig. 7 which relates to the disturbances in the feeding screw. Hence, the consistency and the motor load are not controlled during the trial. This means that the temperature profile together with other process data can be used as inputs to the model when deriving the force distribution between the refining segments. It also gives an opportunity to study the dynamic responses in different temperature sensor elements along the radius.
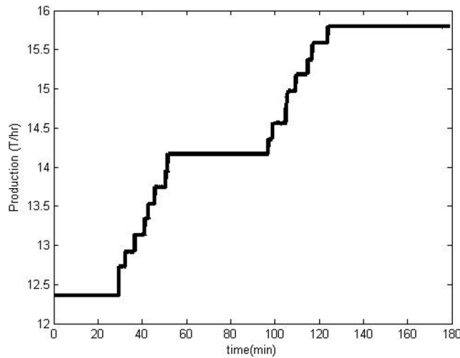
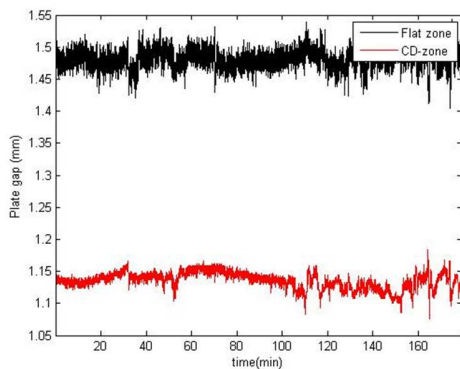*Fig. 6: Step changes in production rate during the test.*

Fig. 7: Plate gap in the flat zone and CD-zone.

The temperature profile is obtained using two sensor arrays, with eight sensors each, mounted between two segments in the refining zones.

As seen in Fig. 8 (upper figure), the increased production rate will result in an increased temperature in all sensor positions along the segment surface. Moreover, the temperature maximum changes position when increasing the production level. A change in the position for the stagnation point of about 100 mm in this specific case will affect the fiber distribution considerably.

In Fig. 8 (lower figure) the temperature profile is also given versus the normalized radius which is defined according to the angle between the flat zone and the CD-zone, see *Fig. 4*. The maximum of the temperature profile can be spatially moved also when changing the dilution water feed rate and the plate gap for this type of refiner as the flat zone and CD-zone are possible to control individually.

It is noteworthy that the sensor position in Fig. 8 should be seen as a length (starting at the inner part of the refining segment in the flat zone followed by the segment in the CD-zone) instead of a radius according to Fig. 3 as normally illustrated in the literature[2].

At high production rates the temperature level will increase in the periphery of the conical zone, see Fig. 9. This is most

---

[2] In this refiner the angle is about 80 °, and this has to be kept in mind when studying the distribution of the work in the flat zone and CD-zone.

likely a consequence of steam evacuation problems. As seen the entire profile is affected by the changes in the production and this can be used in different control concepts, see Eriksson et al. (2010).

As the consistency is allowed to change during the test it is natural to study the consistency profiles for the three production levels, see Fig. 10.

The magnitude of the changes in the consistencies depends on where in the refining zone it is estimated; see Karlström and Eriksson (Part I, 2013). Note variations in the casing pressure directly affect the consistency, both in the casing and the periphery of the CD-zone, while the consistency in the flat zone varies much less. Even though the estimation of the consistency is quite noisy, the trend is clear – the consistency is higher than normal at the highest production level.
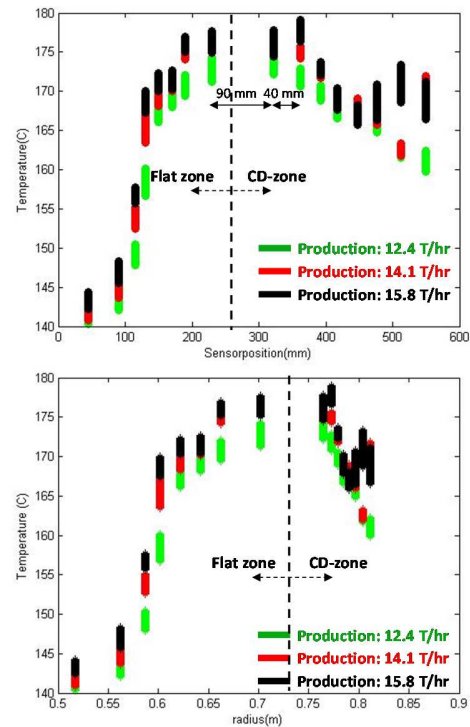

Fig. 8: Upper figure: Temperature profiles vs. actual sensor position on the refining segments at different production levels. The temperature variation in time is seen as vertical lines for each sensor and production level. Lower figure: Temperature profiles vs. normalized radius at different production levels.

From a philosophic perspective it is questionable to use the estimated consistency in the casing if it is affected considerably by the pressure variations in the blow-line.

In production lines where the temperature profile is not measured an enthalpy balance over the refiner is used to estimate the consistency in the casing or the blow-line.

As the temperature profile measurements are available in this paper it is possible to estimate the entire consistency profile and thereby use the inner sensors for consistency control of the CD-zone, see Karlström and Eriksson (Part I, 2013).
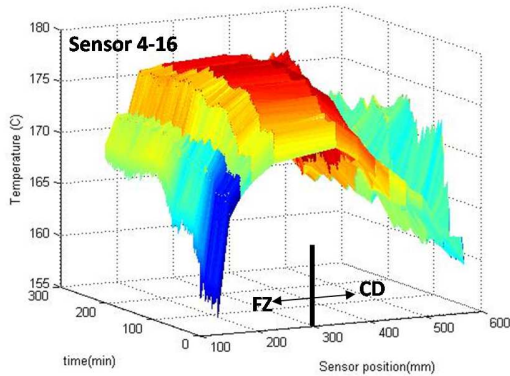

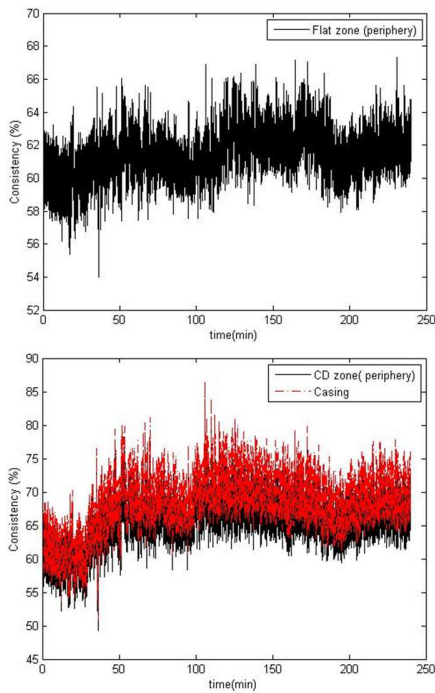*Fig. 9: Temperature profile for sensor 4-16 in the flat zone and CD-zone, respectively.*

Fig. 10: Estimated consistencies in the flat zone, CD-zone and the casing using the extended entropy model.

Defibration/Fibrillation work in the refining zones - As pointed out by Karlström and Eriksson (Part I, 2013) the extended entropy model is suitable for studying the distributed total work in the refining zones.

Using the same terminology as given in Fig. 8 it is easy to understand that the distribution of the total work, i.e. the sum of the thermodynamical and the defibration/ fibrillation work, varies quite much in the CD-zone when the production is increased. As shown in Fig. 11, the distributed total work

in the inner part of the flat zone is not changed to any appreciable account. This is probably a consequence of the open refining segments (in the inner part of flat zone) that are used which allows high production at high consistency.

The distributed total work is higher near the periphery of the segments and increase even further in the CD-zone. This is expected as the plate gaps in both refining zones are kept stable during the test period.
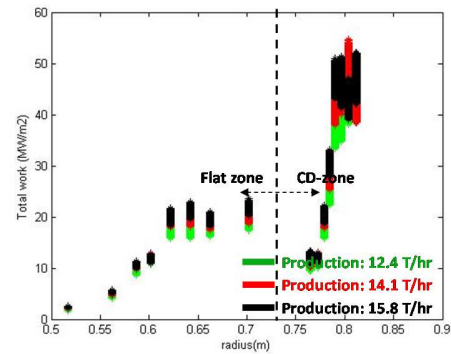

Fig. 11: Distributed total work vs. the normalized radius in the flat zone and CD-zone, respectively.

The minor part of the distributed total work is the defibration/fibrillation work. It is derived as the difference between the total work and the thermodynamical work, see Karlström et al. (2008) and increases when the production level is increased, see Fig. 12.

In many cases the steam production is not considered in details when deriving the bar-to-fiber forces. However, as the free water is assumed to be bounded to the fibers while the major part of the steam is moving in the grooves the defibration and fibrillation work corresponds to the work applied on the pulp and water phases, see Karlström and Eriksson (Part I, 2013).
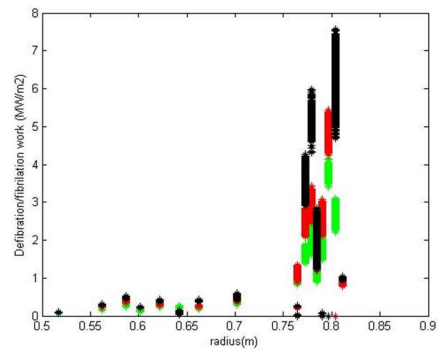

Fig. 12: Defibration/fibrillation work versus the normalized radius in a CD-refiner.

Distributed forces between refining bars - As the irreversible work relates the force distribution in the refining zone, the force on each bar can be estimated according to the

refining segment pattern used, see the example in Fig. 1 and Fig. 2.

For this specific test period the refining segments in the flat zone were quite open while the CD-zone segments had almost the same taper. The bar and groove widths are approximately given in Fig. 13. Note, that the bar and grooves in the flat zone is not symmetric while their widths are more similar in the CD-zone[3].
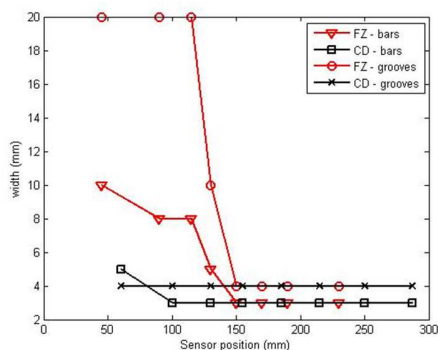

Fig. 13: Width of the bars and grooves in the flat zone and CD-zone, respectively.

Even though the irreversible work distributed in the flat zone, see Fig. 12, seems to be low compared with the irreversible work distribution in the CD-zone, the local force on the bars can be rather high see Fig. 14. This is a consequence of the segment pattern design which together with the temperature profiles, taper and plate gaps give valuable information how the final pulp properties are developed.
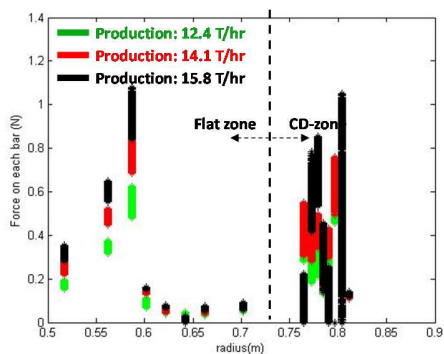

Fig. 14: Forces between fiber bundles and bars versus normalized radius during a production change.

It is notable that the forces on the bars can be zero in the periphery of the CD-zone at high production, see Fig. 14. That is most likely caused by the instability in the fiber pad.

---

[3] In many research reports, the pattern of the refining segments is not mentioned at all even though it has a proven impact on process stability, fiber distribution et cetera. Fortunately in this study, the parameters describing the segment pattern are partly available and possible to include in the entropy model.

In other words, the thermodynamical work approach the total work which means that the fibrillation work approach zero. This can also be interpreted as a limited bar-to-fiber interaction where the major part of the fiber bundle transportation is temporarily performed in the grooves. If a high production is requested, another segment design can be proposed as well in order to avoid local pumping effects.

Using the entropy model, the forces acting on the bars can be seen as elements in an averaged, but still spatially, fiber energy efficiency defined for a number disc revolution[4].

Hence, without knowledge of the temperature profiles in the flat zone and the CD-zone limited information about the bar-to-fiber forces are possible to extract and this may be important to mention as temperature profiles primarily has been used for control purposes so far, see Eriksson et al. (2010).

Comparison between the temperature profile and the motor load - It is easy to understand from the discussion above that the temperature profile contains more information about the refining process than traditional control concepts can capture and future control algorithms can certainly be developed further to include also the force distribution. However, this is not the only extension which can be proposed as the pressure gradient can be derived from the temperature profile as well. The pressure gradient has direct impact on the fiber residence time in different part of the refining zone and knowing the maximum temperature in the flat zone and the CD-zone, the backward and forward steam pressure gradients are possible to control which results in an improved fiber pad stabilization.

Large variations in the temperature profile indicate undesired process conditions in the refining zone. This statement is strengthened by Fig. 15, where the temperature responses for five sensor positions in the CD-zone during the test are given. As seen in the upper figure, the temperature sensor (TCD8) in the outer position of the segment responds to the step change in production before the inner sensor (TCD7) which indicates an abnormal situation. This phenomenon is not detectable by neither the plate gap sensors in Fig. 7 nor the specific energy in Fig. 15. Consequently the local defibration and fibrillation inside the refining zone cannot be detected by using the specific energy or the motor load only. The reason is that the specific energy can be regarded as the integral of the distributed energy along the radius of the segments, i.e. in this paper the flat zone segments and the length of the refining segments in the conical zone. Eriksson and Karlström (2009) also indicated that integrated temperature profiles give similar dynamic information as the motor load at stable production. They did not prove that this relation exists at variable production as given in Fig. 6 and Fig. 15.

---

[4] This is an extension of the concept outlined by Kerekes (2011) where a scalar measure for the refining intensity covering the entire segment surface, was derived.

Hence, if the integrated temperature profile is comparable with the motor load it would be possible to compare how the dynamic information from each temperature sensor contributes to the dynamic response in motor load. This cross-check can be performed by minimizing the difference between the detrended[5] variables representing the motor load and the weighted temperature profile $\Sigma v_n T_n$ in a least square sense using v as a free vector where $\Sigma v_n = 1$; $0 \leq v_n \leq 1$. In this comparison $n=16$ temperature sensors are available for analysis.
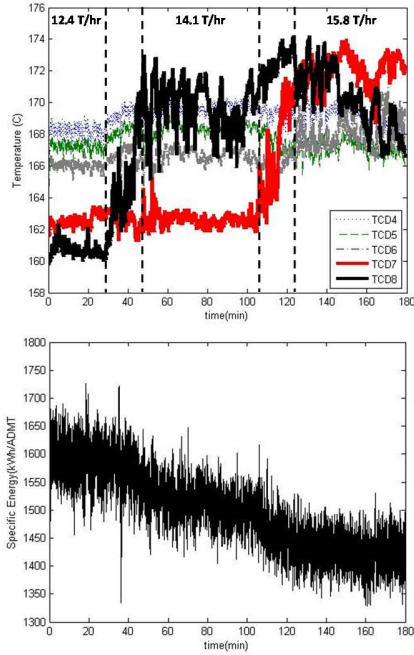

Fig. 15: Upper figure: Temperature responses in four different positions in the CD-zone when changing the production rate. Lower figure: Specific energy response according to changes in the production rate in Fig. 6.

Case I – Increased production: In Fig. 16 (upper figure) the obtained normalized weighting vector, v is given for the data set related to the production changes in Fig. 6.

In Fig. 16 (lower figure) the detrended variables motor load and the sum of the weighted temperature profile are shown and it is interesting to see how the two variables follow each other.

As seen in Fig. 16 the weighting vector has two distinct maxima, one in the flat zone and one in the periphery of the CD-zone. For the flat zone, this can be related to the 3rd sensor that is located in the contraction zone between the rotor and stator segments. In the CD-zone, which has a negligible taper, the responses seem to be more evenly spread over the segments.

Hence, the dynamic responses from the temperature sensors in the contraction zones are of importance when comparing the integrated value with the motor load. It is interesting to see that the changes in production have a minor impact on the prediction. However, it might be possible to improve the estimation even further if the sum of the weighted temperature profile is calculated for each production level. Nevertheless, it is tempting to compare the shape of the weighting vector with the force distribution given in Fig. 14.
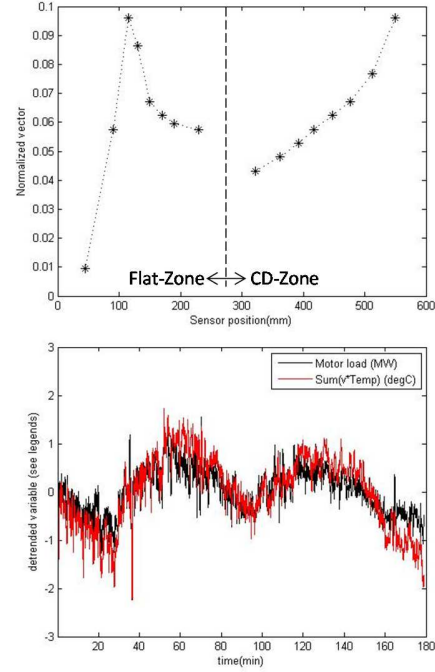

Fig. 16: Upper figure: Weighting vector for the two sensor arrays in the flat zone and CD-zone (in total - 16 sensors), respectively when increasing the production according to Fig. 8. Lower figure: Detrended variables in terms of motor load and the sum of the weighted temperature responses obtained when changing the chip feed rate.

Case II – Reduced plate gap and dilution water in the flat zone: The data set in Fig. 17 is the same detrended data as used by Karlström and Eriksson (Part I, 2013) with two step changes performed in the flat zone plate gap and the dilution water feed rate. As expected the motor load increases when the plate gap and the dilution water flow rate decrease[6]. The changes in the motor load are not sharp which indicates that the fiber pad damps the response when the plate gap and dilution water feed rate changes. As seen in Fig. 17, the plate gap and dilution water changes in the CD-zone are negligible during the trial.

Following the same approach as above it is seen that the maxima of the weighting vector moves outwards in the flat zone for the case when the plate gap is changed, see Fig. 18

---

[5] i.e. the mean value is not included.

[6] To visualize the responses, the plate gap and dilution water flow rate in the flat zone have been multiplied by ten in order to get the same magnitude as the motor load.

(upper figure) while the reduced dilution water feed rate moves the maxima closer to the inner part of the flat zone segment, see Fig. 18 (lower figure). The difference between the two vectors are interesting as the change in the dilution water feed rate does primarily affect the temperature dynamics in the flat zone sensors and not the dynamics in the CD-zone.
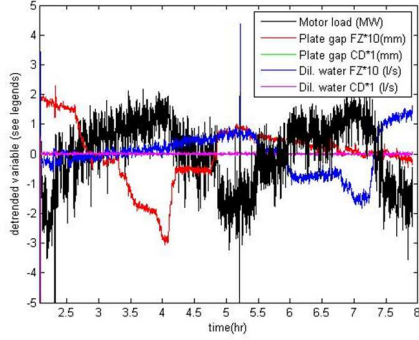

Fig. 17: Detrended variables. Plate gaps and dilution water to the flat zone (FZ) and CD-zone. The plate gap and dilution water feed rate in the CD-zone are overlapped.
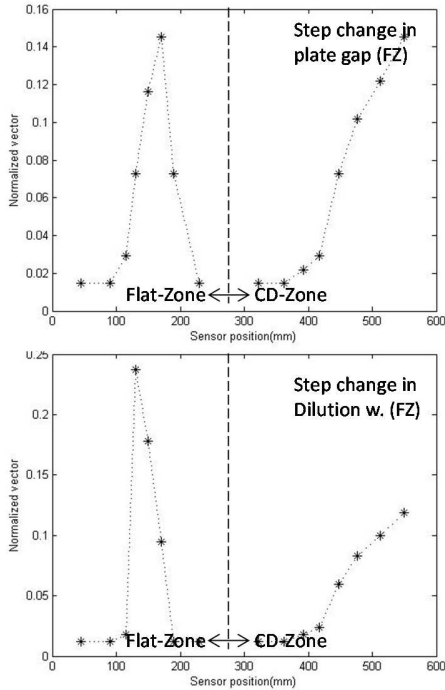

Fig. 18: Weighting vector for the two sensor arrays in the flat zone and CD-zone, respectively. Upper figure: refers to vector obtained when changing the plate gap. Lower figure: refers to the step change in dilution water feed rate to the flat zone (FZ) according to Fig. 17.

In Fig. 19, the detrended variables motor load and the sum of the weighted temperature profile are shown. It is interesting to note that the difference between the motor load and the sum of the weighted temperature profile seems to be harder

to minimize when the dilution water is reduced compared with the case when the plate gap is changed.
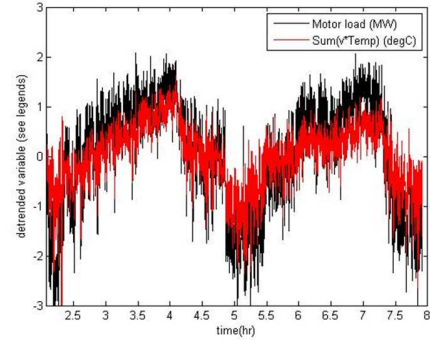

Fig. 19: Detrended variables in terms of motor load and the sum of the weighted temperature response, according to Fig. 17.

To understand the underlying causes some information can be obtained by studying the force distribution in the refining zone, see Fig. 20.
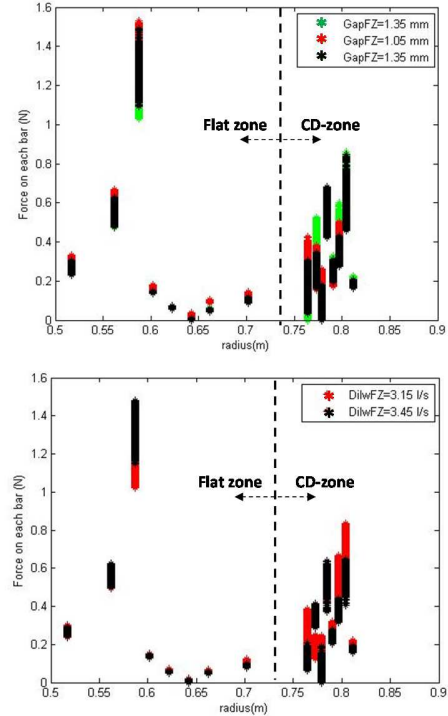

Fig. 20: Forces between fiber bundles and bars versus normalized radius during step changes in (upper figure) the plate gap and (lower figure) the dilution water feed rate to the flat zone.

It is obvious that the force acting on the bars near the 3rd sensor in the flat zone is much higher in Fig. 20 compared with the case given in Fig. 14. The production rate is about 15.3 T/hr, the temperature in the 3rd position is 155 °C and

9

therefore comparable with the high production rate period in Case I see Fig. 14. However, the plate gap in the flat zone is smaller in Case II, see Fig. 7 and Fig. 20, which of course results in a higher force on the bars.

It is also important to note that the forces in the CD-zone for Case II are smaller in magnitude compared with Case I, see Fig. 14 and Fig. 20.

As the forces are related to the local fiber distribution between the segments, the resistance to evacuate steam backwards in the flat zone will be higher in the case described by Fig. 20. This will give a better dynamic response in temperature closer to the centrum in the flat zone and could be one reason why the weighting vectors looks similar to the force distribution in the refining zone.

The responses in the force distribution, when changing the plate gap and the dilution water feed rate in the flat zone, become unclear when plotting it versus the radius in Fig. 20 but as seen in Fig. 21, where the estimated force in the 3rd position is given the responses follow the changes in plate gap and dilution water feed rate.
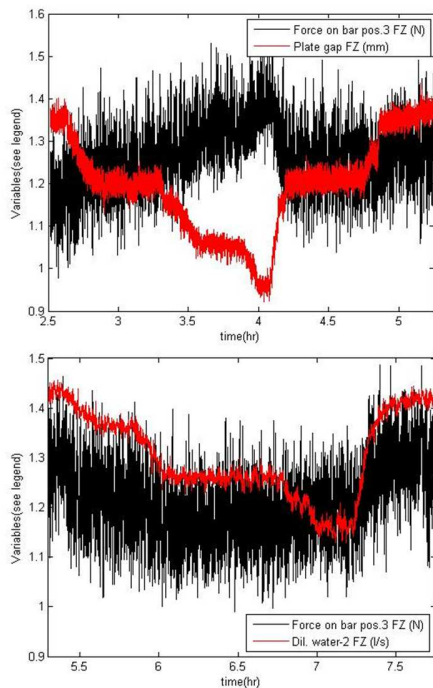

Fig. 21: Forces between fiber bundles and bars versus time during step changes in (upper figure) the plate gap and (lower figure) the dilution water feed rate (-2 l/s) to the flat zone.

When changing the plate gap it is interesting to see that the force will not reach the same level as during the beginning of the test, instead it is slightly higher. Comparing this result with the force between fibers and bars in CD zone (position 15), the force will be reduced, see Fig. 22.
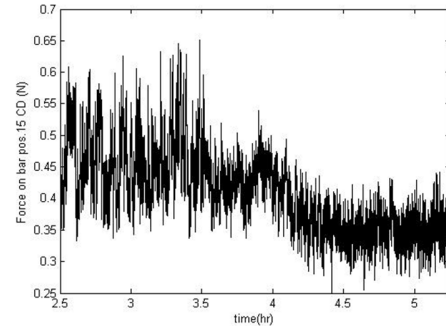

Fig. 22: Forces between fiber bundles and bars in the CD-zone versus time during step changes in the FZ plate gap according to Fig. 21.

Hence, a new fiber distribution is obtained after the step change in plate gap and this phenomenon is described by Rosenqvist et al. (2001) as direction dependent-dynamics which is a non-linear response which often occurs when performing step changes in refiners. This phenomenon is not so well recognized in the pulp and paper industry even though it is mentioned in the research literature and by those who are running the refiners.

Direction dependent dynamics are difficult to see in the force estimation in the 3rd position. However, in the 15th position it is clear, see Fig. 23.

As seen in Fig. 22 and Fig. 23 the forces are lower compared with those given in Fig. 21. However, in both cases the work distribution in the CD-zone become much higher compared with the work in the flat zone and a small change in the flat zone will affect the work distribution in the CD-zone considerably.
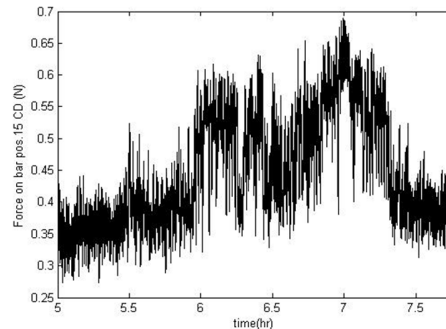

Fig. 23: Forces between fiber bundles and bars in the CD-zone versus time during step changes in the dilution water feed rate to the flat zone according to Fig. 21.

Case III – Step changes in plate gap and dilution water in the CD-zone: When performing step changes in plate gap and the dilution water feed rate to the CD-zone, the weighting vector will be completely different see Fig. 24, compared with the ones in Fig. 16 and Fig. 18.
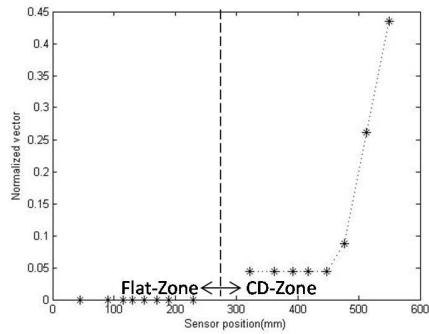
Fig. 24: Weighting vector for the two sensor arrays in the flat zone and CD-zone, respectively.

No changes are performed in the flat zone which can affect the responses in the CD-zone. Also in this case we find that the dynamic response in the motor load can be captured by using the sum of the weighted temperatures in the refining zone, see Fig. 25. Hence, by combining information from the temperature profile similar dynamic information as the motor load (and consequently the specific energy at stable production) is provided.
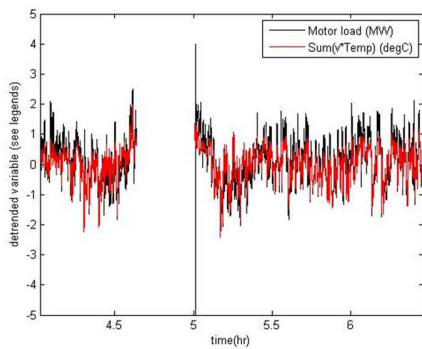

Fig. 25: Detrended variables. Motor load and the sum of the weighted temperature responses when performing step changes in plate gap and dilution water feed rate in the CD-zone

Comments: As seen in Case I-Case III, the sum of the weighted temperature responses in the inner part of the CD-zone when changing production, the plate gaps and the dilution water flow rates, do not add much when searching for a good comparison between the sum of the weighted temperatures and the motor load variations. However, from a process optimization and/or process control perspective the temperature profiles and certainly the maximum temperatures in the flat zone and the CD-zone are of outmost importance as it sets the pressure gradient and thereby the velocity profiles in the refining zone. This will be further discussed in future papers.

From the discussion above we can see that the CD-refiner is indeed a complex system which is affected by many external and internal disturbances, e.g. in the chip quality and feed rate, different operating conditions et cetera. Therefore the analysis is almost impossible to perform by using only the integrated information represented by the motor load or the specific energy. Several local phenomena occur and by measuring the temperature profile or other spatially dependent variables, like e.g. the shear force, in combination with advanced modeling procedures it is possible to derive the forces obtained when the fiber bundles interact with the refining bars. All this will open new ways to approach a deeper understanding of the refining process.

Conclusions

In this paper it is conclude that the difference between the total work and the thermodynamical work in refiners, which is called the irreversible work or the defibration/fibrillation work, can fluctuate significantly.

Using an extended entropy model where the temperature profiles and plate gaps are available for analysis, it is shown that the refining process in a CD-refiner and a Twin refiner are different due to differences in machine and refining segment design as well as in operating conditions. All this affect the distributed defibration/fibrillation work derived.

Moreover, all variables and parameters, significant for the type of refiner, are necessary to include in the model to get a proper estimate of the distributed forces between the refining segments. The distributed forces vary a lot depending on operating conditions. This vector is assumed to give valuable information about the development of the pulp properties and will be penetrated further in future papers by Ferritsius et al (2014).

In this paper it is claimed that the refining intensity as defined by Miles and May (1990, 1991), Kerekes and Senger (2006), Kerekes (2011) and Lundin et al. (2008) should be developed further and not be considered as a scalar nor estimated based on assumed effective coefficients of friction. It is also indicated that the temperature profiles in the flat zone and the CD-zone indirectly coincide with the fiber distribution and depends on process conditions as well as the refining segments structure. Three cases are studied where the temperature profiles are used for comparing the best dynamic fit to the motor load. It is shown that different weighting vectors must be introduced, to cope with the local phenomena inside the refining zones. It is also shown that the shape of the weighting vector distribution seems to follow the force related to the bar-to-fiber interaction. This implies that scalar variables like the specific energy or motor load are too rudimentary and more efforts must be put on research to find better distributed energy efficiency descriptions.

In this paper the concept of fiber energy efficiency is introduced to distinguish between the energy efficiency related to the thermodynamical work and the actual work on the fibers. This indicates that a comprehensive scalar, as often proposed in the refining theory literature, should not be used as a refining intensity measure.

The results presented in this paper open for new on-line applications where the distributed force vector can be used as a tool for analyzing the refining performance. This will be discussed further in coming papers where a micro model for bar-to-fiber interaction is presented.

Acknowledgments

Literature

Atack, D., Stationwala, M. I. and Karnis, A. (1984): What happens in refining, Pulp Paper Can. 85(12), T303.

Backlund, H.-O., Höglund, H. and Gradin, P. (2003): Study of tangential forces and temperature profiles in commercial refiners, Int. Mech. Pulping Conf., Quebec, Canada, 2-5 June 2003, PAPTAC, Montreal, Canada, pp. 379-388.

Batchelor, W.J. and Ouellet, D. (1997): Estimating Forces on Fibres in Refining, 4th PIRA Int. Refining Conf., Fiuggi, Italy.

Brecht, W. and Siewert, (1966): Zur theoretisch-technischen beurteilung des mahlprozesses morderner mahlmaschinen, Papier, 20(1) 4-14.

Dahlqvist G. and Ferrari B. (1981) Mill operating experience with a TMP refiner control system based on a true disc clearance measurement, Int. Mech. Pulping Conf., Oslo, Norway, Session III, no. 6.

Eriksson, K. (2005): An Entropy-based Modeling Approach to Internally Interconnected TMP Refining Processes, Licentiate thesis, Chalmers University of Technology, Göteborg, Sweden.

Eriksson , K., Karlström, A. (2009) Refining zone temperature control: a good choice for pulp quality control? Int. Mech. Pulping Conf. ,Sundsvall, Sweden.

Eriksson, K., and Karlström, A. (2009): Modeling approaches for critical process limitations in the operation of thermomechanical pulp refiners, Nord. Pulp Paper Res. J., 24(2), 231-238.

Eriksson, K., Karlström, A., and Ledung, L. (2010). Controlling TMP refiner lines using pre-specified operating windows, Control Systems Conf., Stockholm, Sweden, 2010.

Eriksen, O., Holmqvist, C. and Mohlin, U-B. (2008): Fibre floc drainage-a possible cause for substantial pressure peaks in low-consistency refiners, Nord. Pulp Paper Res. J., vol 23 no. 3.

Ferritsius, R., Hill, J., Ferritsius, O. and Karlström A. (2014): On energy efficiency in chip refining. Submitted for publication, Int. Mech. Pulping Conf.,June 2-5, Helsinki.

Hill, J., Westin, H., and Bergstrom, R. (1979) Monitoring pulp quality for process control, Int. Mech. Pulping Conf., Toronto, Canada, p. 111-125.

Hill, J., Saarinen, K., Stenros, R.(1993) On the control of chip refining systems, Pulp and Paper Canada, 94(6), p. 43-47.

Honkasalo, J.V., Polkkynen, E.E., Vainio,J.A., (1989) Development of control systems in mechanical pulping (GW, TMP) at Rauma, Int. Mech. Pulping Conf., Helsinki, Finland, p. 376-389

Huhtanen, J.P. (2004): Modeling of Fiber Suspension Flows in Refiner and Other Papermaking Processes by Combining Non-Newtonian Fluid Dynamics and Turbulence, Ph.D. thesis, Tampere University of Technology, Tampere, Finland.

Härkönen, E., Huusari, E. amd Ravila, P.. (1999): Residence time of fibre in a single disc refiner, Int. Mech. Pulping Conf., pp. 77.

Isaksson, A.J., Horch, A., Karlström, A., Allison, B.J and Nilsson, L. (1997): Modelling of mechanical thrust in TMP refiners, Int. Mech. Pulping Conf., p 87-93.

Johansson B.-L., Karlsson H., Jung, E., (1980) Experiences with computer control, based on optical sensors for pulp quality, of a two-stage TMP-plant, 1980 Process Control Conf., Halifax, Nova Scotia, p. 145-152.

Karlström A., Koebe M. (1993) Modelling of wood chip refining processes, Nord. Pulp Paper Res. J. 8(4), p. 384-388.

Karlström, A., Eriksson, K., Sikter, D. and Gustavsson, M. (2008): Refining models for control purposes, Nord. Pulp Paper Res. J., 23(1), 129-138, 2008.

Karlström, A., and Isaksson, A. (2009): Multi-rate optimal control of TMP refining processes, Int. Mech. Pulping Conf., Sundsvall, Sweden.

Karlström, A., (2013): Multi-scale modeling in TMP-processes, 8th Int. Fundamental Mech. Pulp Res. Seminar, Åre, Sweden.

Karlström, A. and Eriksson, K. (2014): Refining energy efficiency Part I: Extended entropy model. Nord. Pulp Paper Res. J.

Karlström, A. and Eriksson, K. (2014): Refining energy efficiency Part III: Modeling of bar-to-fiber interaction. Nord. Pulp Paper Res. J.

Karnis, A., Stationwhala, M.I. and Atack, D. (1985): What happens in refining (part II), Int. Mech. Pulping Conf., pp. 35.

Kerekes, R.J. and Senger, J.J. (2006): Characterizing Refining Action in Low Consistency Refiners by Forces on Fibres, J. Pulp Paper Sci., 32(1), 1-8.

Kerekes, R.J. (2011): Force-based characterization of refining intensity, Nord. Pulp Paper Res. J., Vol 26 no. 1.

Lundin, T., Batchelor, W., Fardim, P. (2008): Fiber Trapping in Low Consistency Refining: New Parameters to Describe the Refining Process, Tappi J., 15-21, July, 2008.

Miles, K. B. and May, W. D. (1990): The Flow of Pulp in Chip Refiners, J. Pulp Paper Sci. 16(2), 63.

Miles, K. B. and May, W. D. (1991): Predicting the performance of a chip refiner: A constitutive approach, Int. Mech. Pulping Conf. p 295-301.

Mohlin, U-B. (2006): Refining Intensity and Gap Clearance, 9th PIRA Int. Refining Conf., No14, Vienna, Austria.

Oksum J., (1983) New technology in the Skogn mechanical pulp mill, Int. Mech. Pulping Conf., Washington DC, USA, p. 143-153.

Rosenqvist, F., Eriksson, K. and Karlström, A. (2001): Time-variant modelling of TMP refining, Advanced Process Control Applications for Industry Workshop, Vancouver, Canada, 2-4 May 2001, IEEE Industry Applications Society, Vancouver, Canada, pp. 37-42.

Sabourin, M., Wiseman, N. and Vaughn, J. (2001): Refining theory considerations for assessing pulp properties in the commercial manufacture of TMP. 55th Appita Annual Conference, p 195-204.

Senger, JJ., Siadat, A., Ouellet, D. and Wild, P. (2004): Measurement of normal and shear forces during refining using a piezoelectric force sensor, J. Pulp Paper Sci., vol 30 no. 9.